Network Connectivity Alterations across the *MAPT* Mutation Clinical Spectrum

Liwen Zhang, PhD,[1] Taru M. Flagan, PhD,[1] Suvi Häkkinen, PhD,[1] Stephanie A. Chu, BS,[1] Jesse A. Brown, PhD,[1] Alex J. Lee, BA,[1] Lorenzo Pasquini, PhD,[1] Maria Luisa Mandelli, PhD,[1] Maria Luisa Gorno-Tempini, MD, PhD,[1] Virginia E. Sturm, PhD,[1] Jennifer S. Yokoyama, PhD,[1] Brian S. Appleby, MD,[2] Yann Cobigo, PhD,[1] Bradford C. Dickerson, MD,[3] Kimiko Domoto-Reilly, MD,[4] Daniel H. Geschwind, MD, PhD,[5] Nupur Ghoshal, MD, PhD,[6] Neill R. Graff-Radford, MD,[7] Murray Grossman, MD,[8] Ging-Yuek Robin Hsiung, MD,[9] Edward D. Huey, MD,[10] Kejal Kantarci, MD,[11] Argentina Lario Lago, PhD,[1] Irene Litvan, MD,[12] Ian R. Mackenzie, MD,[9] Mario F. Mendez, MD, PhD,[5] Chiadi U. Onyike, MD,[13] Eliana Marisa Ramos, PhD,[5] Erik D. Roberson, MD, PhD,[14] Maria Carmela Tartaglia, MD,[15] Arthur W. Toga, PhD,[16] Sandra Weintraub, PhD,[17] Zbigniew K. Wszolek, MD,[7] Leah K. Forsberg, PhD,[11] Hilary W. Heuer, PhD,[1] Bradley F. Boeve, MD,[11] Adam L. Boxer, MD, PhD,[1] Howard J. Rosen, MD,[1] Bruce L. Miller, MD,[1] William W. Seeley, MD,[1] and Suzee E. Lee, MD,[1] on behalf of the ARTFL/LEFFTDS/ALLFTD Consortia

Objective: Microtubule-associated protein tau (*MAPT*) mutations cause frontotemporal lobar degeneration, and novel biomarkers are urgently needed for early disease detection. We used task-free functional magnetic resonance imaging (fMRI) mapping, a promising biomarker, to analyze network connectivity in symptomatic and presymptomatic *MAPT* mutation carriers.
Methods: We compared cross-sectional fMRI data between 17 symptomatic and 39 presymptomatic carriers and 81 controls with (1) seed-based analyses to examine connectivity within networks associated with the 4 most common *MAPT*-associated clinical syndromes (ie, salience, corticobasal syndrome, progressive supranuclear palsy syndrome,

View this article online at wileyonlinelibrary.com. DOI: 10.1002/ana.26738

Received Oct 31, 2022, and in revised form Jun 5, 2023. Accepted for publication Jun 28, 2023.

Address correspondence to Dr S. Lee, UCSF Department of Neurology, Memory and Aging Center, 675 Nelson Rising Lane, MC: 1207, San Francisco, CA 94158, USA. E-mail: suzee.lee@ucsf.edu

From the [1]Memory and Aging Center, Department of Neurology, Weill Institute for Neurosciences, University of California, San Francisco, San Francisco, CA, USA; [2]Department of Neurology, Case Western Reserve University, Cleveland, OH, USA; [3]Department of Neurology, Massachusetts General Hospital and Harvard Medical School, Boston, MA, USA; [4]Department of Neurology, University of Washington, Seattle, WA, USA; [5]Department of Neurology, David Geffen School of Medicine, University of California, Los Angeles, Los Angeles, CA, USA; [6]Departments of Neurology and Psychiatry, Washington University School of Medicine, St Louis, MO, USA; [7]Mayo Clinic, Jacksonville, FL, USA; [8]Perelman School of Medicine, University of Pennsylvania, Philadelphia, PA, USA; [9]University of British Columbia, Vancouver, BC, Canada; [10]Departments of Psychiatry and Neurology, Columbia University, New York, NY, USA; [11]Department of Neurology, Mayo Clinic, Rochester, MN, USA; [12]Department of Neurosciences, University of California, San Diego, La Jolla, CA, USA; [13]Department of Psychiatry and Behavioral Sciences, Johns Hopkins University School of Medicine, Baltimore, MD, USA; [14]Department of Neurology, University of Alabama at Birmingham, Birmingham, AL, USA; [15]Tanz Centre for Research in Neurodegenerative Diseases, Division of Neurology, University of Toronto, Toronto, ON, Canada; [16]University of Southern California, Laboratory of Neuroimaging (LONI), Los Angeles, CA, USA; and [17]Department of Psychiatry and Behavioral Sciences, Mesulam Center for Cognitive Neurology and Alzheimer's Disease, Northwestern Feinberg School of Medicine, Chicago, IL, USA

Additional supporting information can be found in the online version of this article.

and default mode networks) and (2) whole-brain connectivity analyses. We applied K-means clustering to explore connectivity heterogeneity in presymptomatic carriers at baseline. Neuropsychological measures, plasma neurofilament light chain, and gray matter volume were compared at baseline and longitudinally between the presymptomatic subgroups defined by their baseline whole-brain connectivity profiles.

Results: Symptomatic and presymptomatic carriers had connectivity disruptions within *MAPT*-syndromic networks. Compared to controls, presymptomatic carriers showed regions of connectivity alterations with age. Two presymptomatic subgroups were identified by clustering analysis, exhibiting predominantly either whole-brain hypoconnectivity or hyperconnectivity at baseline. At baseline, these two presymptomatic subgroups did not differ in neuropsychological measures, although the hypoconnectivity subgroup had greater plasma neurofilament light chain levels than controls. Longitudinally, both subgroups showed visual memory decline (vs controls), yet the subgroup with baseline hypoconnectivity also had worsening verbal memory and neuropsychiatric symptoms, and extensive bilateral mesial temporal gray matter decline.

Interpretation: Network connectivity alterations arise as early as the presymptomatic phase. Future studies will determine whether presymptomatic carriers' baseline connectivity profiles predict symptomatic conversion.

ANN NEUROL 2023;00:1–15

Pathogenic variants in the microtubule-associated protein tau (*MAPT*) gene cause autosomal dominant frontotemporal lobar degeneration (FTLD).[1] Although behavioral variant frontotemporal dementia (bvFTD) is the most common *MAPT* clinical syndrome, carriers may develop parkinsonism that meets criteria for corticobasal syndrome (CBS) or progressive supranuclear palsy (PSP) syndrome, or develop an amnestic Alzheimer's-like syndrome.[2] Although studies have identified structural changes in both symptomatic and presymptomatic carriers, when neural network alterations, as measured by task-free functional MRI (tf-fMRI), arise remains unclear.

Cross-sectional studies of presymptomatic *MAPT* mutation carriers show either no difference[3,4] or lower[5,6] gray matter volumes, potentially driven by a subset of individuals.[7] Compared to noncarriers, presymptomatic carriers may show subtle differences in cognitive and neuropsychiatric measures[8,9] that are abnormal during the symptomatic phase,[7,10,11] particularly for studies that include carriers with Clinical Dementia Rating (CDR) scores greater than 0.[10,12,13] These findings demonstrate a need for more sensitive markers of symptomatic progression. One promising candidate is tf-fMRI, which detects large-scale intrinsic connectivity networks (ICNs) identifiable in the healthy brain. Neurodegenerative syndromes including bvFTD, CBS, PSP syndrome, and Alzheimer disease (AD) target specific ICNs.[14,15] Presymptomatic carriers of other FTLD genetic mutations, who typically show minimal or no structural brain abnormalities, have shown ICN alterations as extensive as those seen in symptomatic carriers.[4,16–19]

Although no tf-fMRI studies have examined symptomatic *MAPT* mutation carriers, 2 studies with fewer than 10 presymptomatic carriers examined the default mode network (DMN; degenerates in AD) and salience network (SN; degenerates in bvFTD). One study showed DMN hypoconnectivity and hyperconnectivity in presymptomatic carriers compared to controls,[3] whereas the other found no alterations in either network.[4] We hypothesized that our larger cohort would reveal topographically similar alterations in *MAPT*-syndromic ICNs such as the SN and DMN, and additionally the CBS and PSP networks, previously unexamined in *MAPT*. Because greater neuropsychiatric symptoms are associated with reduced SN connectivity in presymptomatic carriers of other FTLD mutations,[17,20] and DMN connectivity is associated with memory performance in patients with dementia,[21] we sought to identify correlations between clinical measures and the SN and DMN.

Here, we studied cross-sectional data to identify connectivity alterations in 17 symptomatic (Sx) and 39 presymptomatic (preSx) *MAPT* mutation carriers. Using seed-based connectivity analyses, we studied 4 ICNs, the SN, CBS and PSP networks, and the DMN, whose regions degenerate in the 4 most common *MAPT*-associated clinical syndromes. Next, correlations between clinical measures and SN and DMN connectivity were examined. We hypothesized that preSx, whose ages spanned from the teens to the 50s, might have heterogeneous connectivity profiles, because older carriers are likelier to be closer to symptomatic onset. To test this hypothesis, we (1) examined the relationship between connectivity and age in these 4 ICNs in preSx versus controls and (2) analyzed whole-brain connectivity to identify heterogeneous profiles within and between 14 ICNs. To determine whether a specific baseline connectivity profile in preSx is associated with indicators of symptomatic conversion, we analyzed baseline and longitudinal differences in neuropsychological measures, neurofilament light chain, a measure of axonal neurodegeneration,[22] and gray matter volume.

Subjects and Methods

Participants

Participants were recruited from the Memory and Aging Center at the University of California, San Francisco, and the Advancing Research and Treatment for Frontotemporal Lobar Degeneration/Longitudinal Evaluation of Familial Frontotemporal Dementia Subjects (ARTFL/LEFFTDS) study.[23] Clinical diagnoses were rendered at each site.

We identified 56 *MAPT* mutation carriers (who tested negative for progranulin variants and the *C9orf72* repeat expansion).[1,24] The 17 Sx included 10 bvFTD, 1 PSP/Richardson syndrome, 1 CBS, 4 mild cognitive impairment, and 1 mild behavioral impairment. The 39 preSx were diagnosed as clinically normal and had a global score = 0 on the CDR plus Behavior and Language domains from the National Alzheimer's Coordinating Center (NACC) FTLD module (CDR plus NACC FTLD).[25] *MAPT* variants included P301L, R406W, V337M, N279K, S305S, S305I, IVS10 + 16C > T, IVS9-10G > T, and G389R. To protect participant anonymity, we do not report sample size for each variant. The P301L group had 17 carriers; each remaining variant group had fewer than 10 carriers. We did not perform variant subgroup analyses due to limited sample sizes.

Given the age difference between carrier groups, 2 healthy control (HC) groups were demographically matched for age, sex, education, and handedness to Sx (46 HC1) and preSx (52 HC2), with an overlap of 17 HCs. These HCs consisted of noncarrier family members and unrelated controls who were included to ensure an age distribution similar to the carriers. All HCs had a Mini-Mental State Examination (MMSE) score ≥ 27 or a corresponding Montreal Cognitive Assessment (MoCA) score ≥ 21[26] and a CDR plus NACC FTLD global score = 0, and no significant history of neurological disease. For all participants, exclusion criteria included (1) significant white matter disease or structural lesions and (2) excessive head motion during MRI acquisition or poor image quality. Participants' medication lists were reviewed for neurological or psychiatric medications.

The neuropsychological battery (tests of executive function, memory, language, and visuospatial functioning) was administered within 180 days of MRI scanning.[17,23] The Neuropsychiatric Inventory Questionnaire (NPI-Q)[27] measured behavioral symptoms and the Geriatric Depression Scale (GDS) assessed depression symptoms.[28] Plasma neurofilament light chain (NfL) levels, a measure of axonal injury, were assayed[29] using the Simoa NF-Light Advantage Kit and the SiMoA HD-X Analyzer instrument. If NfL levels were above the upper limit of the assay, samples were retested at a higher dilution.

For demographics, medication use, and clinical and neuropsychological measures, we conducted linear regression analyses to compare group differences in means (continuous variables) or proportions (categorical variables) for Sx versus HC1, and preSx versus HC2, along with the 95% confidence interval (CI), as measures of effect.

Institutional review boards at each site approved this study, and participants or their surrogates provided informed consent.

Image Acquisition, Preprocessing, and Harmonization

Image acquisition. A 3T MRI scanner at each site collected T1-weighted (T1w) images and a T2*-weighted echo-planar imaging sequence.[17,23] All participants completed a tf-fMRI session of either 240 volumes in 8:08 min, or 197 volumes in 10 min, depending on the scanning site.

fMRI preprocessing. fMRI data were preprocessed using the fMRIPrep pipeline and in-house scripts (Nipype v1.2.1).[30] Briefly, the T1w image was corrected for intensity nonuniformity, skull-stripped, segmented, and spatially normalized to MNI standard space through nonlinear registration (Advanced Normalization Tools [ANTs]).

The first 5 fMRI volumes were dropped for magnetic field stabilization. A reference volume and its skull-stripped version were generated using a custom methodology of "fMRIPrep," then coregistered to the T1w reference using boundary-based registration with six degrees of freedom. Blood oxygen level-dependent (BOLD) data were corrected for slice-timing, head-motion, and susceptibility distortions. Motion-correcting transformations, BOLD-to-T1w transformation, and T1w-to-MNI warp were concatenated and applied in a single step (antsApplyTransforms, ANTs; Lanczos interpolation). Data were smoothed with a 3-dimensional 6mm full width at half maximum Gaussian kernel. Subsequently, we applied nonaggressive ICA-AROMA[31] to identify and regress independent components representing motion-related artifacts. Finally, BOLD time series underwent linear detrending, bandpass filtering (0.008∼0.08Hz), and nuisance regression (Friston's 24 motion parameters, mean signals from white matter, cerebrospinal fluid [CSF], and global signal). Participants with inaccurate segmentation or registration, or excessive head motion, were excluded from further analyses. Excessive head motion was defined as (1) mean framewise displacement throughout the acquisition of >0.5mm or (2) having less than a total of 4 minutes of data without large motion spikes (ie, >0.5mm framewise displacement).[32]

Structural MRI processing. Structural images were preprocessed with longitudinal voxel-based morphometry following previous methods.[33] Each participant's structural image was first segmented into different tissue types based on standard prior tissue probability maps (eg, gray matter, white matter, and CSF). An average template was then created using serial longitudinal registration, and the structural image for each visit was warped into the average template space. The average template was segmented with standard prior tissue probability maps and normalized into MNI standard space. After that, all structural images were warped from the average template space to MNI standard space using the deformation parameters estimated from the previous step, modulated by multiplying the Jacobian determinant to account for individual brain volumes. Gray matter maps were smoothed with an 8mm full width at half maximum isotropic Gaussian kernel. Next, these gray matter maps were parcellated into 246 regions of interest (ROIs) based on the Brainnetome atlas, and gray matter

volume within each ROI was obtained for subsequent statistical analyses.

Harmonization. As a postacquisition data harmonization strategy for structural[34] and fMRI data,[35] we applied a customized ComBat approach by removing batch effects of no interest (eg, different scanners), while preserving biological variability of interest (ie, age, sex, education, and handedness). ComBat parameters were estimated in an independent HC group (119 HC3; Table S2) whose demographic and imaging characteristics spanned the age range and scanner sites of the study cohorts (ie, carriers, HC1, and HC2), and used to harmonize study cohort data. For structural MRI analyses, ComBat was applied on the smoothed gray matter maps prior to parcellation into the 246 ROIs. For fMRI analyses, ComBat was applied as described below.

Seed-Based Connectivity Analyses

Figure 1 lists the analysis overview schematic. We used a seed-based connectivity approach to examine ICNs associated with the 4 most common *MAPT*-associated clinical syndromes: bvFTD, CBS, PSP syndrome, and an Alzheimer's-like syndrome. We created a 4mm-radius sphere (the "seed") around peak atrophy coordinates based on patients with the corresponding clinical syndrome from literature[15,36] (Table S1) to identify the SN (targeted in bvFTD), the CBS and PSP syndrome networks, and the DMN (targeted in an Alzheimer's-like syndrome). Using SPM12, connectivity was assessed using bivariate regression between the mean BOLD time series within each seed and the time series in the remaining voxels, resulting in 4 ICN maps per participant. ComBat was then applied to individual ICN maps.

For each ICN, general linear models compared Sx versus HC1 and preSx versus HC2 cross-sectionally. To explore whether connectivity alterations might be driven by older preSx presumably closer to symptom onset, we used age by group interaction models for each network to identify voxels in which the slopes of connectivity versus age differed in preSx versus HC2.

We built separate regression models to identify relationships between ICNs and clinical measures. We searched for SN voxels that were negatively correlated with GDS scores, and DMN voxels that were positively correlated with verbal memory (California Verbal Learning Test [CVLT] 10-minute recall) or visual memory (Benson figure recall) scores. Due to insufficient data, we did not test the relationship between SN connectivity and NPI-Q scores. We analyzed all carriers combined, then each carrier group.

These voxelwise seed-based connectivity analyses used a voxel-level height threshold of $p < 0.05$ and a cluster-extent threshold of $p < 0.05$ for multiple comparison correction at the whole-brain level, following previous publications[16,17,20,37] and masked to the relevant network (Fig 2). Network masks were created by using 1-sample t tests of seed-based ICN maps of HC3, thresholded at $t \geq 4$. Age, sex, education, handedness, and eyes-open status during MRI scanning ("eyes-open status" hereafter) were included as nuisance covariates.

Whole-Brain Connectivity Analyses

Intranetwork and Internetwork Connectivity

We used a whole-brain approach to study connectivity cross-sectionally within all nodes of a network (intranetwork connectivity) and between different networks (internetwork connectivity). Briefly, the brain was parcellated into 246 Brainnetome atlas-based ROIs, which were grouped into 14 networks.[38] These 14 networks included bilateral frontoparietal, cingulo-opercular, salience, subcortical, anterior temporal, hippocampal, parahippocampal, amygdala, DMN, dorsal attention, auditory, sensory motor, and visual networks. Individual 246×246 connectivity matrices, in which connectivity between each pair of ROIs was calculated as a z-transformed Pearson correlation, were constructed then harmonized with ComBat. Diagonal values were set to zero. For each ROI, we calculated intranetwork connectivity, the mean connectivity of each ROI to every other ROI from the same network, and internetwork connectivity, the mean connectivity to each ROI from each of the remaining networks. For each network, we calculated an intranetwork connectivity composite score by averaging the intranetwork connectivity for all ROIs within that network, and internetwork connectivity composite scores by averaging the internetwork connectivity for each pair of networks. This calculation yielded 14 intranetwork and 91 internetwork connectivity composite scores per participant, which were used for the subsequent analyses on the network level.

We compared intranetwork or internetwork connectivity composite scores between (1) Sx and HC1 and (2) preSx and HC2 using multiple linear regression (R v4.0.3), regressing age, sex, education, handedness, and eyes-open status. False discovery rate (FDR) was applied to correct for multiple comparisons (105 measures, $p_{FDR} < 0.05$).

Clustering Analysis and Subgroup Comparisons. To explore whether preSx might have heterogeneous connectivity profiles, we performed K-means clustering based on the 105 whole-brain intra−/internetwork connectivity measures. We used the silhouette coefficient to determine the optimal number of clusters, and set 50 random starting assignments and 100 maximum iterations to select the best clustering results. We did not perform clustering analyses in Sx due to the limited sample size. For visualization only, we conducted a principal component analysis of the same 105 connectivity measures, then plotted the preSx

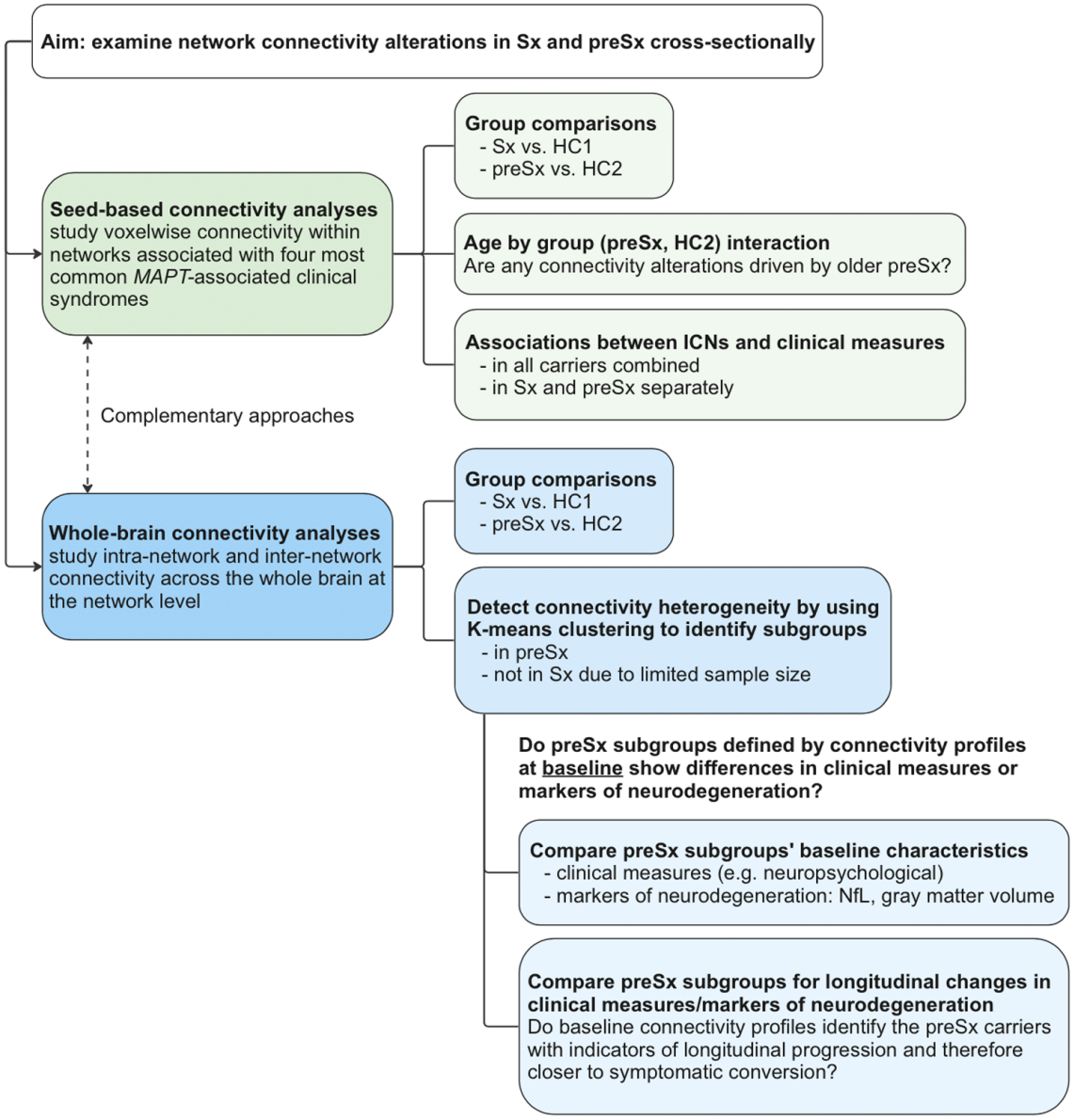

FIGURE 1: Analysis overview schematic. Two complementary analytical connectivity approaches are utilized to study network connectivity alterations in Sx and preSx. The seed-based approach examines connectivity within ICNs in association with the 4 most common *MAPT*-associated clinical syndromes. Connectivity levels are compared between carriers and matched controls. To explore whether connectivity alterations might be driven by older preSx presumably closer to symptom onset, age by group (preSx and HC2) interaction analyses are performed. Additionally, association between clinical measures and ICNs are examined, including correlations between salience network connectivity and depressive symptoms and between default mode network connectivity and memory performance based on previous studies of frontotemporal dementia. The whole-brain connectivity approach studies connectivity within and between 14 ICNs encompassing regions across the brain. Because preSx consist of a mixture of some carriers closer than others to symptom onset, we explore whole-brain connectivity heterogeneity in preSx. To determine whether a specific whole-brain connectivity profile at baseline identifies presymptomatic carriers who may be closer to symptom onset, we characterize the clinical measures and markers of neurodegeneration at baseline and longitudinally in preSx subgroups. HC2 = healthy controls matched to presymptomatic carriers; ICN = intrinsic connectivity network; NfL = neurofilament light chain; preSx = presymptomatic *MAPT* mutation carriers; Sx = symptomatic *MAPT* mutation carriers.

subgroups defined by K-means clustering along the first 2 principal components.

Using linear regression (in-house R scripts), we compared the presymptomatic subgroups (defined by the K-means clustering based on whole-brain connectivity) and HC2 for cross-sectional differences in intra−/internetwork connectivity, neuropsychological measures, and neurodegeneration markers (NfL and gray matter volume). For group comparisons of each intra−/internetwork connectivity measure, we regressed age, sex, education,

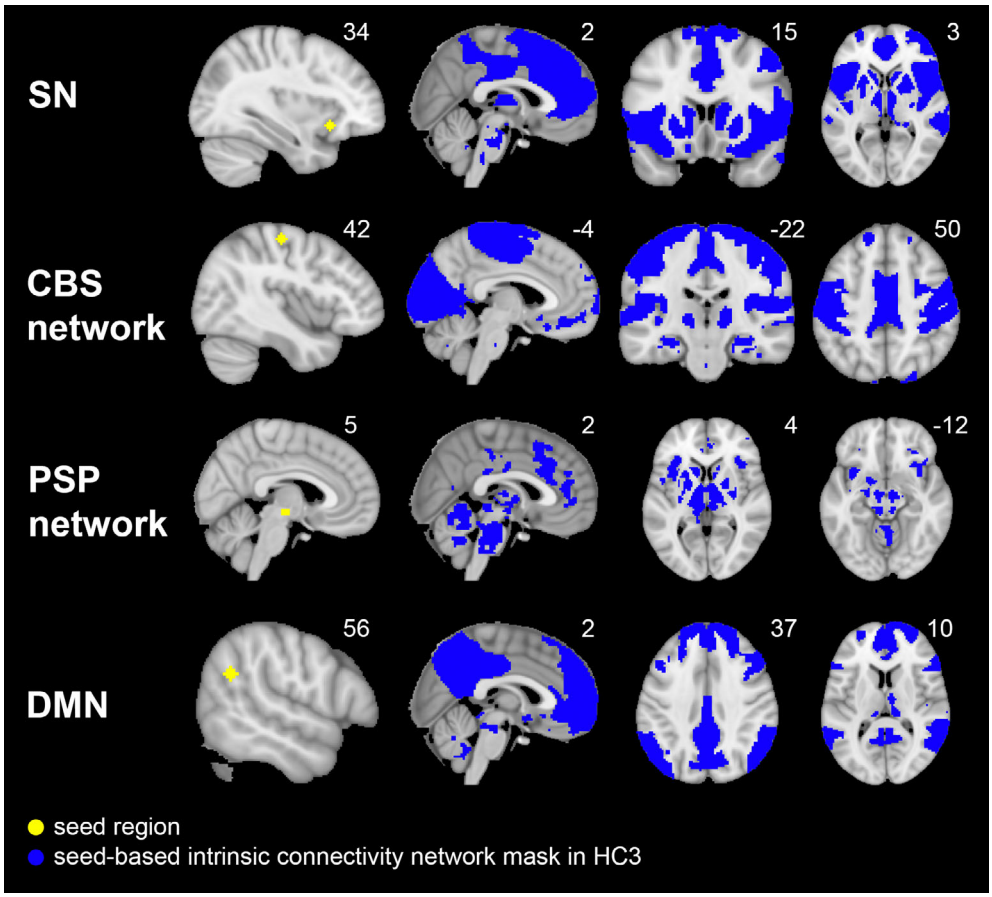

FIGURE 2: Seed-based intrinsic connectivity networks associated with the 4 most common *MAPT-associated* clinical syndromes. Using peak atrophy regions from previous literature as seed regions (yellow), 4 networks of interest (blue) are derived in an independent healthy control group (ie, 119 HC3). These networks include the SN, which degenerates in behavioral variant frontotemporal dementia, the CBS and PSP syndrome networks, and the DMN for an Alzheimerlike syndrome. These network maps were used as masks to constrain subsequent seed-based analyses. CBS = corticobasal syndrome; DMN = default mode network; HC3 = independent healthy control group for multisite image data harmonization; PSP = progressive supranuclear palsy; SN = salience network.

handedness, and eyes-open status, applying FDR correction (105 measures, $P_{FDR} < 0.05$). NfL data were available in a subset (31 preSx, 40 HC2) and were compared by log-transforming the data and including age and sex as covariates, along with simultaneous 95% CI, using a Bonferroni correction, as measures of effect. For comparisons of regional gray matter volume, we regressed age, sex, education, handedness, and total intracranial volume, applying FDR correction for the 246 ROIs ($p_{FDR} < 0.05$).

To probe whether the cross-sectional (baseline) connectivity profiles may identify presymptomatic carriers who may be closer to symptomatic conversion, we compared the presymptomatic subgroups, defined by K-means clustering based on whole-brain connectivity profiles at baseline, to determine whether a specific subgroup had indicators of longitudinal progression. Specifically, we compared longitudinal changes in neuropsychological measures, NfL levels, and regional gray matter volume between presymptomatic subgroups and HC2, using separate linear mixed models. Analyses thresholded at $p_{FDR} < 0.05$. For all linear mixed models, fixed effects included group, time between baseline and follow-up, group by time interaction, age, sex, education (for neuropsychological measures and gray matter only), handedness (gray matter only), and total intracranial volume (gray matter only). Random effects included individual intercepts and the slope of time. We used linear regression to compare presymptomatic subgroups for their proportions of longitudinal symptomatic converters, along with the 95% CI.

This study's data are available upon reasonable request.

Results

Neuropsychological Testing

As expected, Sx (vs HC1) had lower scores on the MMSE, MoCA, and CDR plus NACC FTLD (Table 1),

Table 1. Demographics of *MAPT* mutation carriers and matched controls

	HC1 ($n = 46$)	Sx-*MAPT* ($n = 17$)	Beta, 95% CI	Test statistic, p	HC2 ($n = 52$)	preSx-*MAPT* ($n = 39$)	Beta, 95% CI	Test statistic, p
Age (years)	59.0 (13.5)	54.4 (11.9)	4.56, [−2.9, 12]	$t(61) = 1.23$, 0.225	40.6 (12.5)	37.3 (11.9)	3.3, [−1.8, 8.5]	$t(89) = 1.28$, 0.204
Education (years)	16.7 (2.6)	15.4 (1.9)	1.26, [−0.1, 2.7]	$t(61) = 1.81$, 0.076	15.5 (2.6)	15.5 (2.8)	0, [−1.1, 1.1]	$t(89) = 0$, 1
Sex (% Female)	23 (50.0%)	7 (41.2%)	−0.09, [−0.1, 0.3]	$\chi^2 = 0.39$, 0.534	34 (65.4%)	20 (51.3%)	0.14, [−0.06, 0.3]	$\chi^2 = 1.84$, 0.175
Handedness, R/L	42/4	16/1	–0.03, [−0.4, 0.3]	$\chi^2 = 0.13$, 0.714	47/5	36/3	−0.02, [−0.4, 0.3]	$\chi^2 = 0.103$, 0.749
Neurological or psychiatric medications (% Yes)	8 (17.4%)	8 (47.1%)	−0.3, [−0.6, −0.04]	$\chi^2 = 5.77$, 0.016*	10 (19.2%)	8 (20.5%)	-0.01, [−0.3, 0.2]	$\chi^2 = 0.02$, 0.879
CDR® plus NACC FTLD, global score	0 (0)	1.29 (0.81)	−1.29, [−1.5, −1.1]	$t(61) = -10.97$, <0.001*	0 [0,0]	0 [0,0]	-	-
CDR® plus NACC FTLD, sum of boxes	0 (0)	6.29 (5.1)	−6.29, [−7.8, −4.8]	$t(61) = -8.45$, <0.001*	0 (0)	0 (0)	-	-
MMSE, total score	29.3 (0.8)	21.1 (8.7)	8.2, [5, 11.4]	$t(36) = 5.26$, <0.001*	28.6 (0.9)	29.4 (0.5)	−0.8, [−1.5, −0.15]	$t(26) = -2.51$, 0.019*
MoCA, total score	27.5 (2.6)	20.2 (7.5)	7.3, [3.7, 10.9]	$t(32) = 4.12$, <0.001*	27.4 (2.1)	27.5 (2.3)	−0.1, [−1.1, 0.9]	$t(75) = -0.16$, 0.871
Clinical syndromes							-	
bvFTD	-	10			-	-	-	
MBI	-	1			-	-	-	
MCI	-	4			-	-	-	
PSP	-	1			-	-	-	
CBS	-	1			-	-	-	

Note: Table 1 presents differences in the mean values (continuous variables) or proportions (categorical variables) from comparisons between carrier group to demographically matched control group, along with the 95% CI as measures of effect. Mean (SD) values are reported for continuous variables, unless otherwise indicated.

Abbreviations: bvFTD = behavioral variant frontotemporal dementia; CBS = corticobasal syndrome; CDR® plus NACC FTLD = CDR® Dementia Staging Instrument plus Behavior and Language domains from the National Alzheimer's Coordinating Center (NACC) Frontotemporal Lobar Degeneration Module; HC1 = healthy controls matched to symptomatic carriers; HC2 = healthy controls matched to presymptomatic carriers; MBI = mild behavioral impairment; MCI = mild cognitive impairment; MMSE = Mini-Mental State Examination; MoCA = Montreal Cognitive Assessment; preSx-*MAPT* = presymptomatic *MAPT* mutation carriers; PSP = progressive supranuclear palsy; Sx-*MAPT* = symptomatic *MAPT* mutation carriers; 95% CI = 95% confidence intervals. *$p < 0.05$.

impairments in all cognitive domains, and greater neuropsychiatric symptoms (NPI-Q) and depression (GDS) (Table 2). PreSx had a slightly higher MMSE score versus HC2, and no other differences.

Symptomatic and Presymptomatic Carriers Showed Alterations in MAPT*-Syndromic Networks*

Seed-based connectivity analyses showed that Sx predominantly showed disruptions (ie, lower connectivity) within *MAPT*-syndromic ICNs (Fig 3, Table S3). SN connectivity disruptions emerged in bilateral anterior cingulate, superior medial prefrontal and inferior frontal gyri and supplementary motor area, right superior frontal gyrus, temporal and parietal cortex, bilateral insula, right striatum, and thalamus. CBS hypoconnectivity arose in bilateral perirolandic cortex and precuneus, along with a small region of hyperconnectivity principally in the left cerebellum extending to the fusiform gyrus. Sx showed a right frontal region of DMN hypoconnectivity. Sx had no PSP connectivity alterations. PreSx versus HC2 had connectivity disruptions in all 4 networks (see Fig 3, Table S4). Regions of SN hypoconnectivity mirrored those of Sx, namely in bilateral striatum and thalamus. CBS connectivity disruptions emerged in bilateral occipital regions, and PSP hypoconnectivity arose in bilateral thalami. PreSx had DMN disruptions in bilateral angular gyrus, and DMN hyperconnectivity in right temporal cortex.

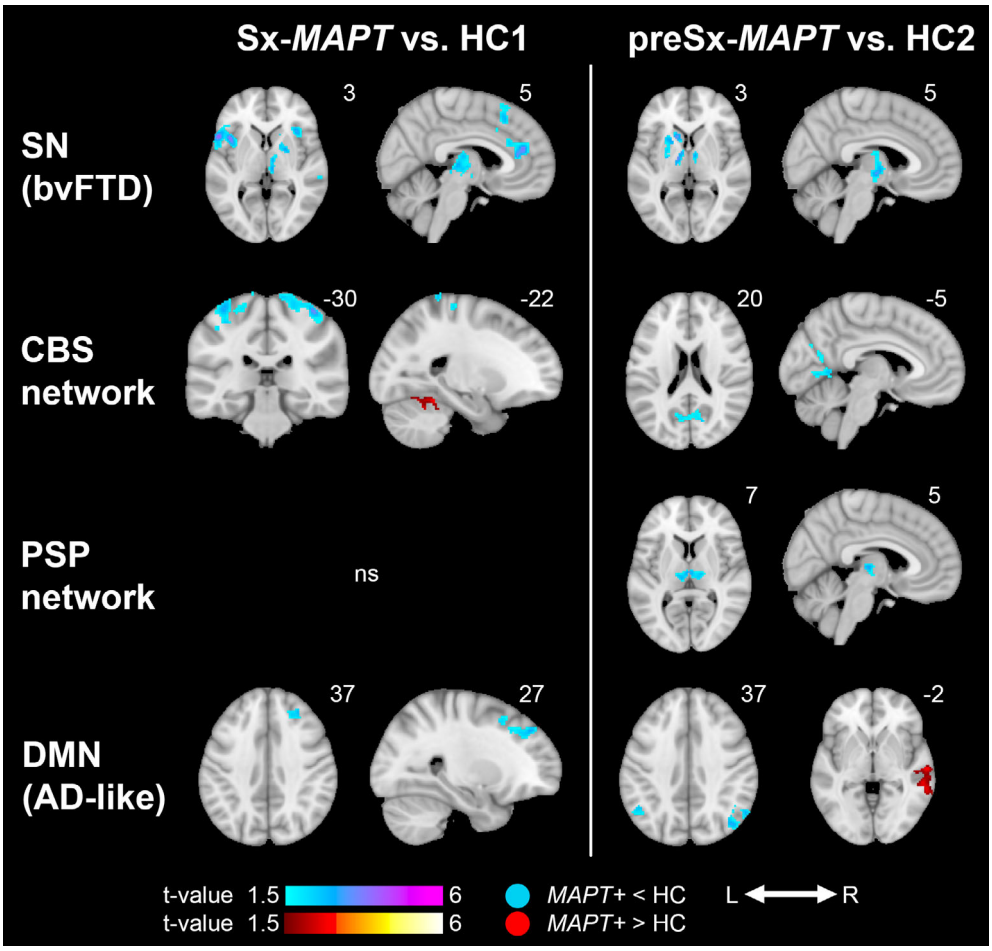

FIGURE 3: Sx-*MAPT* and preSx-*MAPT* show functional connectivity alterations in networks associated with *MAPT*-related clinical syndromes. (Left panel) Group contrast maps predominantly show connectivity disruptions in Sx-*MAPT* compared to HC1 for all networks of interest except for the DMN. (Right panel) PreSx-*MAPT* have connectivity disruptions within all networks compared to HC2. Results are thresholded at a joint height and extent threshold of $p < 0.05$, masked to the relevant network, and superimposed on the Montreal Neurological Institute brain template. Color bars represent *t* values. AD = Alzheimer disease; bvFTD = behavioral variant frontotemporal dementia; CBS = corticobasal syndrome; DMN = default mode network; HC1 = healthy controls matched to symptomatic carriers; HC2 = healthy controls matched to presymptomatic carriers; *MAPT*+ = *MAPT* mutation carriers; ns = not significant; preSx-*MAPT* = presymptomatic *MAPT* mutation carriers; PSP = progressive supranuclear palsy syndrome; SN = salience network; Sx-*MAPT* = symptomatic *MAPT* mutation carriers.

For cross-sectional group by age interaction analyses, preSx (vs HC2) had regions of lower connectivity with age within key hubs of the SN (bilateral anterior/mid cingulate, superior medial prefrontal cortex, and right dorsolateral prefrontal cortex) and the CBS network (bilateral perirolandic and occipital cortex), alongside higher DMN connectivity in bilateral temporal and parietal regions (Fig 4). No differences were identified in the relationship between PSP connectivity and age.

In PreSx, Symptoms of Depression and Worse Memory Were Associated with Lower Connectivity in SN and DMN, Respectively

PreSx showed correlations between clinical measures and ICNs within key network hubs. Specifically, higher GDS scores (greater symptoms of depression) correlated with lower SN connectivity in bilateral anterior/mid cingulate and right supramarginal/superior temporal gyrus (Fig 5). Lower Benson figure recall scores (visual memory) correlated with lower connectivity in bilateral medial prefrontal cortex, mid/posterior cingulate, precuneus, and left lateral temporoparietal cortex. There was no positive correlation between CVLT 10-minute recall (verbal memory) and DMN.

Sx showed no relationships between these clinical measures and ICNs. In all carriers combined, higher GDS scores correlated with lower SN connectivity in a small region of the left supramarginal/superior temporal gyrus, and there were no positive correlations between memory scores and DMN connectivity (Table S5).

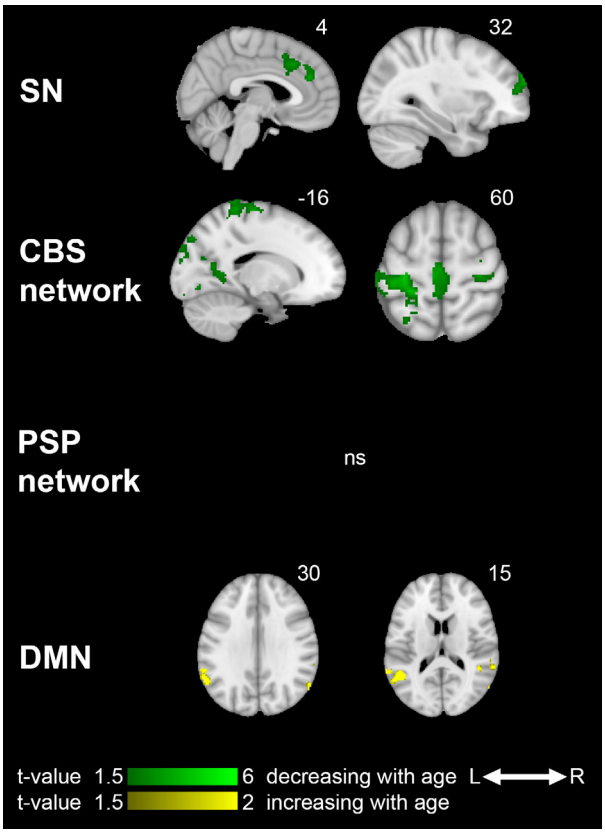

FIGURE 4: Cross-sectional functional connectivity changes with age in preSx-*MAPT*. Colored brain regions depict the interaction between age and group on connectivity in networks associated with *MAPT*-related clinical syndromes. PreSx-*MAPT* show regions of lower (green) and higher (yellow) connectivity with increasing age compared to HC2. Results are thresholded at a joint height and extent threshold of $p < 0.05$, masked to the relevant network, and superimposed on the Montreal Neurological Institute brain template. Color bars represent *t* values. CBS = corticobasal syndrome; DMN = default mode network; HC2 = healthy controls matched to presymptomatic carriers; ns = not significant; preSx-*MAPT* = presymptomatic *MAPT* mutation carriers; PSP = progressive supranuclear palsy syndrome; SN = salience network.

Clustering Analyses Identified Presymptomatic Subgroups That Exhibited Predominantly Either Hypoconnectivity or Hyperconnectivity

In contrast to the seed-based connectivity analyses, we found no intra−/internetwork connectivity alterations for either carrier group (all $p_{FDR} > 0.05$). We speculated that this whole-brain ROI-based approach could dilute differences in regions smaller than the Brainnetome ROIs, and might be less sensitive for detecting group differences, particularly if there were heterogeneity across individuals within a given region.

To assess whether preSx have heterogeneous connectivity profiles, we applied K-means clustering based on participants' intranetwork and internetwork connectivity measures and identified 2 subgroups (Fig 6A). We did not analyze Sx due to its limited sample size. Unthresholded connectivity difference matrices predominantly showed either whole-brain hypoconnectivity (28 preSx1 vs HC2) or hyperconnectivity (11 preSx2 vs HC2 or preSx1; see Fig 6B, top row), and statistical comparisons revealed significant differences for select networks (see Fig 6B, bottom row).

Longitudinal Declines in Clinical Measures and Gray Matter in Presymptomatic Carriers

Because preSx1 predominantly featured connectivity disruptions (hypo-preSx1), as did Sx, we hypothesized that hypo-preSx1 might show baseline or longitudinal differences in neuropsychological or neurodegeneration measures compared to preSx2 with predominant hyperconnectivity (hyper-preSx2) and/or HC2. At baseline, there were no differences in demographics, neuropsychological measures, regional gray matter volumes, or *MAPT* mutation subtype frequency between the presymptomatic subgroups and HC2 (Table S6). Hypo-preSx1 had higher NfL levels compared to HC2 ($p = 0.019$, 95% CI = −0.2 to −0.006); there were no differences between hyper-preSx2 and HC2, or between presymptomatic subgroups.

Hypo-preSx1 and hyper-preSx2 had no differences in longitudinal follow-up intervals or number of visits for neuropsychological measures, NfL, or first and last MRI scans (Table S6). At follow-up, 4 of 28 hypo-preSx1 and 1 of 11 hyper-preSx2 converted to the symptomatic phase ($\chi^2 = 0.19$, $p = 0.662$, 95% CI = −0.3 to 0.5). Both presymptomatic subgroups had longitudinal decline in the Benson figure recall (hypo-preSx1 vs HC2, $t[15.03] = -3.38$, $p = 0.004$, 95% CI = −1 to −0.2; hyper-preSx2 vs HC2, $t[29.31] = -4.12$, $p < 0.001$, 95% CI = −1.5 to −0.5), and a longitudinal increase in the CDR plus NACC FTLD global score (hypo-preSx1 vs HC2, $t[207.12] = 7.7$, $p < 0.001$, 95% CI = 0.08 to 0.1; hyper-preSx2 vs HC2, $t[148.5] = 6.1$, $p < 0.001$, 95% CI = 0.07 to 0.1) and sum of boxes score (hypo-preSx1 vs HC2, $t[201.58] = 6.29$, $p < 0.001$, 95% CI = 0.3 to 0.5; hyper-preSx2 vs HC2, $t[151.0] = 6.5$, $p < 0.001$, 95% CI = 0.5 to 0.9). Hypo-preSx1 (vs HC2) additionally showed longitudinal decline in the CVLT 10-minute recall ($t[32.32] = -2.23$, $p = 0.033$, 95% CI = −0.6 to −0.04) and increase in the NPI-Q score ($t[135.67] = 1.98$, $p = 0.0495$, 95% CI = 0.02 to 1.1). Direct subgroup comparisons showed no differences. There were no significant group differences in longitudinal NfL levels.

Compared to HC2, hypo-preSx1 had bilateral insula and widespread longitudinal mesial temporal volume decline, whereas hyper-preSx2 showed less extensive temporal volume decline (Fig 7). When compared directly, presymptomatic subgroups had no differences in

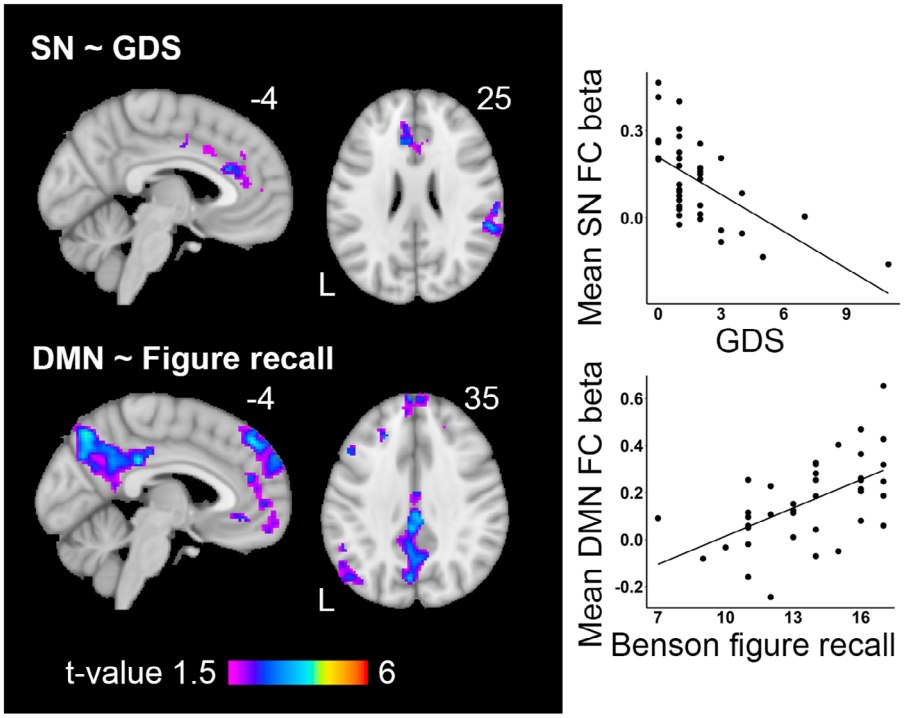

FIGURE 5: In preSx-*MAPT*, symptoms of depression and lower memory scores are associated with lower connectivity in the SN and DMN, respectively. (Top row) In preSx-*MAPT*, voxelwise regression analyses show regions of lower SN connectivity in association with higher GDS scores (reflective of greater symptoms of depression). (Bottom row) Lower Benson figure recall (visual memory) is associated with regions of lower DMN connectivity. Dot plots on the right of each map indicate the mean ICN connectivity beta values within the significant regions for each subject. Results are thresholded at a joint height and extent threshold of $p < 0.05$, masked to the relevant network, and superimposed on the Montreal Neurological Institute brain template. Color bars represent *t* values. Beta parameters extracted from significant clusters are plotted versus clinical variables of interest. DMN = default mode network; FC = functional connectivity; GDS = Geriatric Depression Scale; preSx-*MAPT* = presymptomatic *MAPT* mutation carriers; SN = salience network.

longitudinal gray matter decline. Although the presymptomatic subgroups had no differences in longitudinal follow-up time, 3 hypo-preSx1 individuals had data available for longer than the maximum follow-up time for hyper-preSx2 (ie, 5.12 years). To determine whether these 3 participants may be influencing the results, we performed an analysis in which we included only time points for hypo-preSx1 that were within 5.12 years. For each group, the regions of longitudinal gray matter decline (data not shown) were comparable to the original analysis that included all time points.

Discussion

In this study, we identified connectivity alterations within the seed-based *MAPT*-syndromic networks in both Sx and preSx. Compared to controls, preSx had connectivity alterations associated with age in key hubs within the SN, CBS network, and DMN, which resembled the connectivity alterations in Sx. In preSx, lower SN and DMN connectivity were associated with greater depressive symptoms and lower visual memory scores, respectively. Based on whole-brain connectivity analyses, we identified 2 distinct presymptomatic subgroups. The subgroup with predominant hypoconnectivity (vs HC2) showed signs of neurodegeneration both cross-sectionally (NfL levels) and longitudinally (extensive longitudinal gray matter decline). These findings suggest that preSx show ICN changes with age and that they have heterogeneous connectivity profiles that may signal the symptomatic phase.

Symptomatic and Presymptomatic Carriers Have Connectivity Alterations within MAPT*-Syndromic Networks*

To our knowledge, this is the first tf-fMRI study of symptomatic *MAPT* mutation carriers. Consistent with our hypothesis, Sx had key cortical regions of connectivity disruptions in the SN, CBS network, and DMN, which revealed network failure during the symptomatic phase. In contrast to our finding of DMN hypoconnectivity, some studies of bvFTD have found DMN hyperconnectivity in cortical hubs (eg, angular gyrus or precuneus) alongside hypoconnectivity in varying regions,[37,39] whereas others

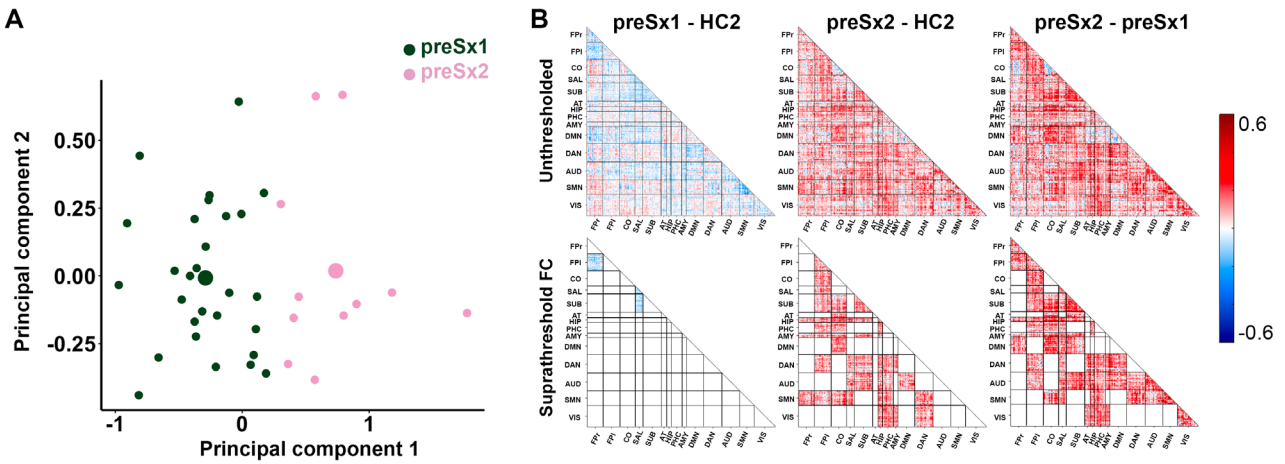

FIGURE 6: Clustering analysis based on whole-brain connectivity measures identifies presymptomatic subgroups with heterogeneous connectivity profiles. (A) K-Means clustering based on whole-brain intranetwork and internetwork connectivity measures yields 2 preSx-*MAPT* subgroups. For post hoc visualization only, a principal component analysis based on the same whole-brain connectivity measures is conducted, and the 2 subgroups defined by K-means clustering are plotted along the 2 principal components that explain the most variance (PC1 vs PC2). (B) Visualization of whole-brain connectivity difference matrices between these preSx-*MAPT* subgroups and matched HC2 shows that preSx1 predominantly have hypoconnectivity (blue color scale) and preSx2 predominantly have hyperconnectivity (red color scale) both before (top row) and after (bottom row) between-group statistical comparisons ($p_{FDR} < 0.05$). Statistical comparisons were performed at the network level, whereas nodal connectivity strengths are plotted for visualization only. The network labels from left/top to right/bottom are: FPr, FPl, CO, SAL, SUB, AT, HIP, PHC, AMY, DMN, DAN, AUD, SMN, and VIS. AMY = amygdala network; AT = anterior temporal network; AUD = auditory network; CO = cingulo-opercular network; DAN = dorsal attention network; DMN = default mode network; FC = functional connectivity; FDR = false discover rate; FPl = left frontoparietal network; FPr = right frontoparietal network; HC2 = healthy controls matched to presymptomatic carriers; HIP = hippocampal network; PC = principal component; PHC = parahippocampal network; preSx1 = subgroup 1 of presymptomatic *MAPT* mutation carriers; preSx2 = subgroup 2 of presymptomatic *MAPT* mutation carriers; preSx-*MAPT* = presymptomatic *MAPT* mutation carriers; SAL = salience network; SMN = sensory motor network; SUB = subcortical network; VIS = visual network.

show hyperconnectivity only[40,41] or its absence.[42] These studies consisted of participants principally with sporadic disease or unknown genetic mutation status, in contrast to our Sx group. In contrast to sporadic bvFTD, *MAPT*-bvFTD show impaired episodic memory in association with hippocampal atrophy.[7] Because the mesial temporal lobe participates in the DMN, whose proposed functions include episodic memory,[43,44] we propose that mesial temporal involvement in *MAPT* may lead to DMN disruption.

Similar to Sx, the whole preSx group had connectivity disruptions within all 4 seed-based ICNs. In preSx, one study found divergent DMN connectivity patterns and no SN connectivity alterations,[3] whereas another showed no connectivity alterations in either the SN or DMN.[4] This discrepancy may be attributable to sample size differences (<10 vs 39 preSx in the present study). As in studies of other FTLD mutations,[16,20] our results suggest that tf-fMRI network analysis shows promise for capturing disease-related alterations from the presymptomatic to symptomatic phases.

In line with the literature,[17,20,21] greater symptoms of depression and lower memory scores in preSx were associated with SN and DMN disruption, respectively. Although these clinical measures did not differ between preSx and HC2, these correlations suggest that in preSx, reduced SN and DMN connectivity may indicate incipient clinical decline. We did not find such correlations in Sx. One explanation is that Sx possess significant memory impairment and depressive symptoms (see Table 2), resulting in limited dynamic ranges for these variables. Additionally, Sx had a smaller sample size (n = 17) compared to preSx (n = 39), which may have limited statistical power to detect clinical–ICN correlations.

Connectivity Relationships with Age in Presymptomatic Carriers: A Sign of Impending Symptomatic Onset?

Compared to controls, preSx showed regions with decreases (seed-based SN and CBS network) and increases (seed-based DMN) in connectivity with age. Interestingly, key network hubs of the SN (anterior cingulate/medial prefrontal cortex) and CBS network (bilateral perirolandic cortex) that showed steeper declines with age in preSx (see Fig 4) were also the regions that appeared as hypoconnective in Sx (see Fig 3). This finding suggests that these age-associated SN and CBS network declines in preSx may signal the symptomatic phase. Similarly, bilateral parietal regions of the DMN, which showed increasing connectivity with age, were regions of hypoconnectivity in preSx

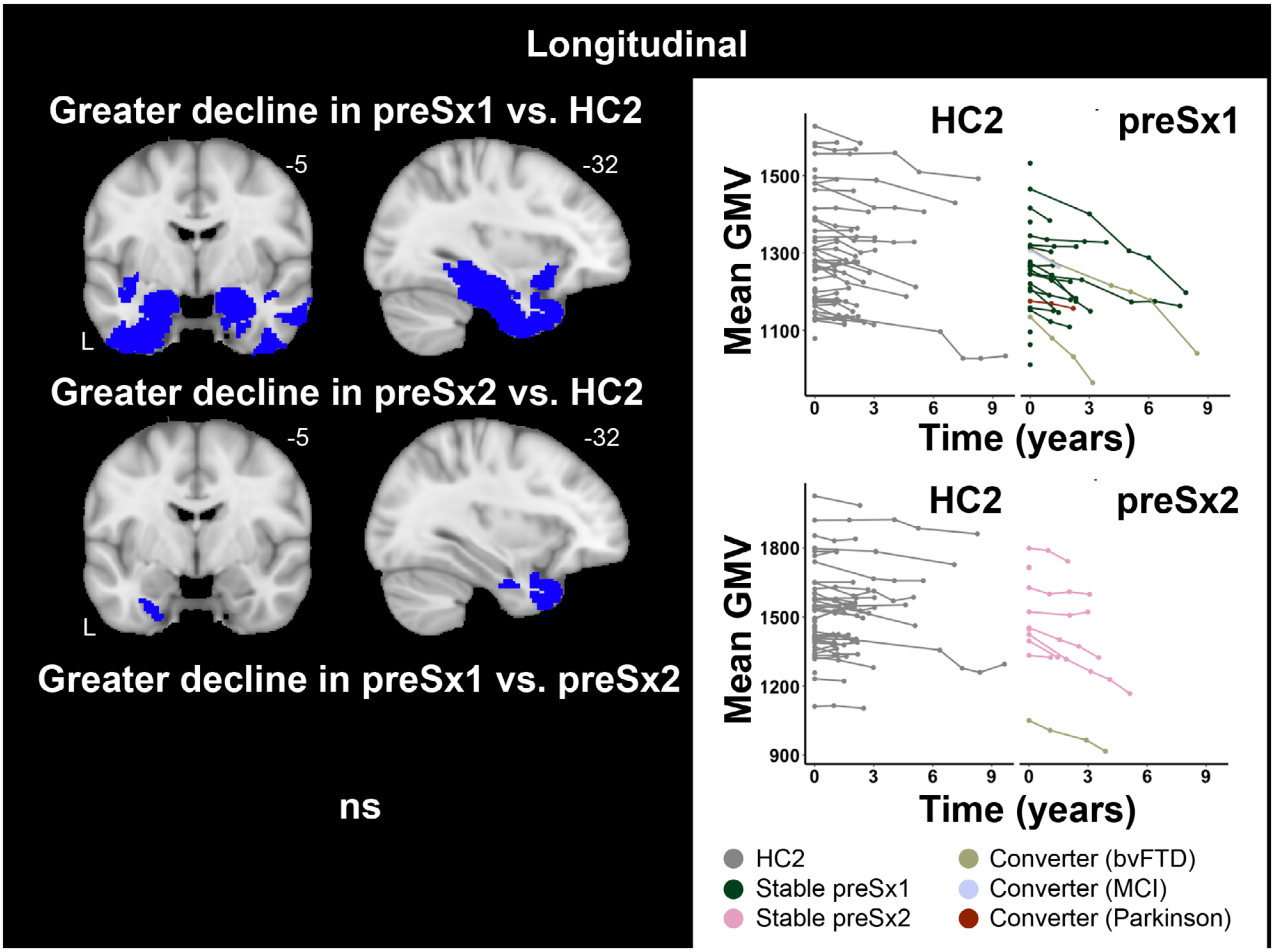

FIGURE 7: Longitudinal GMV decline in presymptomatic subgroups. Compared to HC2, preSx1 has extensive regions of longitudinal GMV decline in bilateral mesial temporal cortex, anterior temporal pole, and insula, whereas preSx2 shows longitudinal volume decline in the left anterior temporal pole and fusiform. Line plots show each preSx-*MAPT* carrier's mean GMV over time within those regions, showing significant longitudinal decline compared to HC2. Each carrier was defined as preSx-*MAPT* at baseline, and the clinical diagnoses at each participant's last visit are annotated by different colors. Cross-sectional comparisons of regional gray matter showed no significant group differences between presymptomatic subgroups and controls. All maps are superimposed on the Montreal Neurological Institute brain template. bvFTD = behavioral variant frontotemporal dementia; GMV = gray matter volume; HC2 = healthy controls matched to presymptomatic carriers; MCI = mild cognitive impairment; ns = no significant regions; preSx1 = presymptomatic carrier subgroup 1 defined by whole-brain connectivity-based clustering; preSx2 = presymptomatic carrier subgroup 2 defined by whole-brain connectivity-based clustering; preSx-*MAPT* = presymptomatic *MAPT* mutation carriers.

but not in Sx, suggesting that DMN hypoconnectivity found in these regions during the presymptomatic stage may attenuate by the symptomatic phase. It remains unclear whether this age-associated DMN connectivity may serve as a compensatory mechanism during the presymptomatic phase. Taken together, these results suggest that network alterations, driven by older preSx, presumably closer to symptom onset, may herald the symptomatic phase. Of note, our preSx ranged from the teens to the 50s, and it remains unclear to what extent the ICN alterations identified represent neurodevelopmental differences. Although it is unknown to what extent *MAPT* mutations are associated with neurodevelopmental differences in humans, it has been long known that tau expression changes dynamically during neurodevelopment.[45] In the fetal brain, high levels of phosphorylated tau protein have been observed, hypothesized to enhance structural neuroplasticity in the developing brain.[46] Future studies are needed to explore whether *MAPT* mutations influence network connectivity during brain development.

Presymptomatic Carriers Show Divergent Network Connectivity Profiles

A clustering analysis identified 2 presymptomatic subgroups predominantly exhibiting either whole-brain hypoconnectivity (hypo-preSx1) or hyperconnectivity (hyper-preSx2). Because Sx predominantly showed connectivity disruptions, we hypothesized that hypo-preSx1 may show signs of approaching the

Table 2. Neuropsychological measures of *MAPT* mutation carriers and matched controls

	HC1 ($n = 46$)	Sx-*MAPT* ($n = 17$)	Beta, 95% CI	Test statistic, p	HC2 ($n = 52$)	preSx-*MAPT* ($n = 39$)	Beta, 95% CI	Test statistic, p
NPI-Q, total score	0.8 (1.1)	6.2 (4.2)	−5.4, [−7.6, −3.2]	$t(27) = -5.03$, <0.001*	1.1 (2.1)	1.7 (3.0)	−0.6, [−1.9, 0.6]	$t(67) = -1.04$, 0.303
GDS-15, total score	0.8 (1.4)	2.8 (2.3)	−2, [−3, −1]	$t(57) = -4.0$, <0.001*	1.5 (1.9)	1.9 (2.1)	−0.4, [−1.2, 0.4]	$t(88) = -0.94$, 0.349
Trails A, correct lines per minute	62.3 (17.7)	41.8 (19.9)	20.5, [9.2, 31.8]	$t(49) = 3.63$, <0.001*	73.7(25.4)	79.8 (24.3)	−6, [−17.3, 5.2]	$t(77) = -1.07$, 0.288
Trails B, correct lines per minute	28.3 (9.4)	19.7 (11.9)	8.6, [2.1, 15]	$t(48) = 2.68$, 0.01*	31.0 (11.5)	31.7 (11.7)	−0.7, [−5.9, 4.6]	$t(77) = -0.26$, 0.797
Digit span forward	7.1 (1.1)	6.3 (1.7)	0.8, [0.02, 1.6]	$t(50) = 2.05$, 0.045*	7.1 (1.04)	7.1 (1.3)	−0.01, [−0.5, 0.5]	$t(86) = -0.05$, 0.963
Digit span backward	5.6 (1.2)	4.7 (1.7)	0.9, [0.08, 1.8]	$t(52) = 2.2$, 0.032*	5.6 (1.3)	5.9 (1.4)	−0.3, [−0.8, 0.3]	$t(88) = -0.88$, 0.379
Semantic fluency, animals in 1 min	23.1 (5.2)	14.3 (8.2)	8.8, [5.2, 12.5]	$t(55) = 4.89$, <0.001*	23.6 (5.5)	23.5 (5.8)	0.1, [−2.3, 2.5]	$t(89) = 0.07$, 0.945
Lexical fluency, words in 1 min	27.3 (8.8)	20.4 (11.0)	6.9, [−0.2, 14]	$t(31) = 1.99$, 0.055	28.6 (7.7)	31.6 (10.8)	−3, [−7.2, 1.3]	$t(74) = -1.39$, 0.167
Delayed free recall (CVLT-short, 10 min recall)	6.8 (2.0)	3.71 (3.4)	3.1, [1.3, 4.9]	$t(33) = 3.41$, 0.002*	7.4 (1.6)	7.1 (1.5)	0.3, [−0.4, 1]	$t(85) = 0.87$, 0.385
Benson figure 10 min recall, total score	12.0 (2.8)	9.2 (5.5)	2.8, [0.6, 5.0]	$t(55) = 2.57$, 0.013*	13.0 (2.3)	13.7 (2.6)	−0.7, [−1.7, 0.3]	$t(89) = -1.32$, 0.191
Multilingual Naming Test, total score	29.4 (2.7)	22.8 (7.6)	6.6, [2.8, 10.3]	$t(31) = 3.58$, 0.0012*	29.5 (2.4)	29.4 (2.5)	0.1, [−1, 1.2]	$t(74) = 0.17$, 0.867
Benson figure copy, total score	15.4 (1.3)	15.1 (1.2)	0.3, [−0.4, 1]	$t(55) = 0.82$, 0.415	15.8 (1.1)	16.0 (1.0)	−0.2, [−0.7, 0.2]	$t(89) = -1.06$, 0.293

Note: Table 2 presents differences in the mean values (continuous variables) or proportions (categorical variables) from comparisons between carrier group to demographically matched control group, along with the 95% CI as measures of effect. Mean (SD) values are reported for continuous variables, unless otherwise indicated.

Abbreviations: CVLT = California Verbal Learning Test; GDS = Geriatric Depression Scale; HC1 = healthy controls matched to symptomatic carriers; HC2 = healthy controls matched to presymptomatic carriers; NPI-Q = Neuropsychiatric Inventory–Questionnaire; preSx-*MAPT* = presymptomatic *MAPT* mutation carriers; Sx-*MAPT* = symptomatic *MAPT* mutation carriers; 95% CI = 95% confidence intervals. *$p < 0.05$.

symptomatic stage. Thus, we compared baseline and longitudinal neuropsychological measures, and NfL and gray matter in hypo-preSx1, hyper-preSx2, and HC2. We identified no significant group differences in baseline neuropsychological measures, or gray matter volumes, although hypo-preSx1 had greater NfL than HC2. Consistent with studies of presymptomatic FTLD mutation carriers,[3,4,16,17] these results demonstrate that tf-fMRI connectivity alterations predate significant gray matter loss also in *MAPT*.

Both presymptomatic subgroups (vs controls) had longitudinal visual memory decline and increasing symptom severity. Hypo-preSx1 additionally showed longitudinal verbal memory decline and worsening neuropsychiatric symptoms compared to controls, although there were no longitudinal differences in neuropsychological measures between hypo-preSx1 and hyper-preSx2. These results suggest that memory and neuropsychiatric symptoms are sentinel measures of decline in preSx. Previous studies have also noted verbal memory decline in presymptomatic *MAPT* mutation carriers in addition to declines in language, social cognition, and visuoconstruction.[8,9]

Although the presymptomatic subgroups had no gray matter abnormality at baseline, hypo-preSx1 (vs controls) showed bilateral insula and extensive regions of longitudinal bilateral mesial temporal decline compared to those seen in hyper-preSx2. This result reveals that whole-brain network connectivity profiling at a baseline time point without atrophy identifies a group of preSx with greater longitudinal gray matter decline at future time points. These longitudinal gray matter declines involved the insula and the mesial temporal lobe, regions that degenerate in symptomatic carriers[7,47,48] and decline in longitudinal studies of presymptomatic carriers.[49,50] In sum, these results indicate that for preSx, hypoconnectivity at baseline may point to neurodegeneration at future time points.

Limitations and Future Directions

Across the major disease-causing FTLD genetic variants, *MAPT*, *GRN*, and *C9orf72*, tf-fMRI mapping identifies ICN abnormalities in presymptomatic carriers prior to significant atrophy.[3,4,16–18] A limitation of our preSx data is that the majority have an unknown symptomatic onset. Thus, longitudinal studies are needed to confirm whether preSx with hypoconnectivity are at greater risk for impending symptomatic conversion. Due to limited sample sizes, we did not examine connectivity for *MAPT* variant subtypes. Overall, our results highlight the importance of considering individual differences to understand the biology of these disorders and variation in the trajectories of clinical and imaging biomarkers.

Author Contributions

L.Z. and S.E.L. contributed to the conception and design of the study. The ARTFL/LEFFTDS/ALLFTD Consortia contributed to data acquisition, and L.Z., S.H., T.M.F., S.A.C., J.A.B., A.J.L., W.W.S., and S.E.L. contributed to analysis of data. All authors contributed to manuscript writing.

Acknowledgments

This work was supported by the following agencies: the Tau Consortium (S.E.L., N.G., A.L.B., W.W.S.), Päivikki and Sakari Sohlberg Foundation (S.H.), and NIH (J.A.B.: K01AG055698 [NIA]; L.P.: K99-AG065457 [NIA], R00AG065457 [NIA]; M.L.G.-T.: R01NS050915 [NINDS], K24DC015544 [NIDCD]; V.E.S.: R01AG052496 [NIA]; D.H.G.: P30AG062422-03 [NIA], P01AG019724 [NIA]; N.G.: U01AG045390-01A1 [NIA], U54NS092089-01 [NINDS], K12 HD001459 [NICHD]; M.G.: AG066597 [NIA]; E.D.H.: R01MH120794 [NIMH], R01AG062268 [NIA]; K.K.: P30 AG062677 [NIA]; I.L.: 2R01AG038791-06A [NIA], U01NS100610 [NINDS], R25NS098999 [NINDS], U19 AG063911-1 [NIA], 1R21NS114764-01A1 [NINDS]; S.W.: P30 AG072977 [NIA]; N.G./I.R.M./B.F. B./A.L.B./H.J.R.: U19AG063911 [NIA]; A.L.B.: R01AG038791 [NIA]; B.L.M.: P30AG062422 [NIA], P01AG019724 [NIA], R01AG057234 [NIA]; S.E.L.: R01 AG058233 [NIA], R01AG071756 [NIA]). K.D.-R. receives research funding from Lawson Health Research Institute and receives speaker payment from MedBridge. N.G. also receives funding from the Association for Frontotemporal Dementia. G.-Y.R.H. is supported by the Ralph Fisher Professorship in dementia research from the Alzheimer Society of British Columbia. I.L. is also supported by the Michael J. Fox Foundation, Parkinson Foundation, Lewy Body Association, CurePSP, Roche, Abbvie, Biogen, Centogene, EIP-Pharma, Biohaven Pharmaceuticals, Novartis, and United Biopharma SRL–UCB. I.R.M. also received research support from the CIHR (74580) and the Alzheimer's Association. A.L.B. also receives research support from the Association for Frontotemporal Degeneration, Bluefield Project to Cure Frontotemporal Dementia, Alzheimer's Drug Discovery Foundation, and Alzheimer's Association.

Data collection and dissemination of the data in this article were supported by the ARTFL-LEFFTDS Longitudinal Frontotemporal Lobar Degeneration: a multisite research consortium [ALLFTD Consortium] (U19: AG063911, funded by the NIH National Institute on Aging [NIA] and NIH National Institute of Neurological Diseases and Stroke [NINDS]) and the former ARTFL and LEFFTDS Consortia (ARTFL: U54 NS092089, funded by the NINDS and NIH National Center for Advancing Translational Sciences; LEFFTDS: U01 AG045390, funded by the NIA and NINDS). Samples from the National Centralized Repository for Alzheimer's Disease and Related Dementias, which receives support under a cooperative agreement grant (U24AG021886) awarded by the NIA, were used in this study.

The authors acknowledge the invaluable contributions of the study participants and families as well as the assistance of the support staff at each of the participating sites. The manuscript was reviewed by the Publications Committee of ARTFL/LEFFTDS for scientific content.

Potential Conflicts of Interest

Nothing to report.

References

1. Hutton M, Lendon CL, Rizzu P, et al. Association of missense and 5J-splice-site mutations in tau with the inherited dementia FTDP-17. Nature 1998;393:702–705.
2. Moore KM, Nicholas J, Grossman M, et al. Age at symptom onset and death and disease duration in genetic frontotemporal dementia: an international retrospective cohort study. The Lancet Neurology 2020;19:145–156.
3. Whitwell JL, Josephs KA, Avula R, et al. Altered functional connectivity in asymptomatic MAPT subjects: a comparison to bvFTD. Neurology 2011;77:866–874.
4. Dopper EGP. Structural and functional brain connectivity in presymptomatic familial frontotemporal dementia. Neurology 2013;80:814–823.
5. Rohrer JD, Nicholas JM, Cash DM, et al. Presymptomatic cognitive and neuroanatomical changes in genetic frontotemporal dementia in the genetic frontotemporal dementia initiative (GENFI) study: a cross-sectional analysis. The Lancet Neurology 2015;14:253–262.
6. Cash DM, Bocchetta M, Thomas DL, et al. Patterns of gray matter atrophy in genetic frontotemporal dementia: results from the GENFI study. Neurobiol Aging 2018;62:191–196.
7. Chu SA, Flagan TM, Staffaroni AM, et al. Brain volumetric deficits in *MAPT* mutation carriers: a multisite study. Ann Clin Transl Neurol 2021;8:95–110.
8. Jiskoot LC, Dopper EGP, Heijer T, et al. Presymptomatic cognitive decline in familial frontotemporal dementia: A longitudinal study. Neurology 2016;87:384–391.

9. Jiskoot LC, Panman JL, van Asseldonk L, et al. Longitudinal cognitive biomarkers predicting symptom onset in presymptomatic frontotemporal dementia. J Neurol 2018;265:1381–1392.
10. Poos JM, Russell LL, Peakman G, et al. Impairment of episodic memory in genetic frontotemporal dementia: a GENFI study. Alz & Dem Diag Ass & Dis Mo 2021;13:e12185.
11. Samra K, Macdougall A, Peakman G, et al. Neuropsychiatric symptoms in genetic frontotemporal dementia: developing a new module for clinical rating scales. J Neurol Neurosurg Psychiatry 2023;94:357–368.
12. Cheran G, Wu L, Lee S, et al. Cognitive indicators of preclinical behavioral variant frontotemporal dementia in *MAPT* carriers. J Int Neuropsychol Soc 2019;25:184–194.
13. Cheran G, Silverman H, Manoochehri M, et al. Psychiatric symptoms in preclinical behavioural-variant frontotemporal dementia in *MAPT* mutation carriers. J Neurol Neurosurg Psychiatry 2018;89:449–455.
14. Seeley WW, Crawford RK, Zhou J, et al. Neurodegenerative diseases target large-scale human brain networks. Neuron 2009;62:42–52.
15. Gardner RC, Boxer AL, Trujillo A, et al. Intrinsic connectivity network disruption in progressive supranuclear palsy: network disruption in PSP. Ann Neurol 2013;73:603–616.
16. Lee SE. Network degeneration and dysfunction in presymptomatic C9ORF72 expansion carriers. NeuroImage: Clinical 2017;14:286–297.
17. Lee SE, Sias AC, Kosik EL, et al. Thalamo-cortical network hyperconnectivity in preclinical progranulin mutation carriers. NeuroImage: Clinical 2019;22:101751.
18. Borroni B, Alberici A, Cercignani M, et al. Granulin mutation drives brain damage and reorganization from preclinical to symptomatic FTLD. Neurobiol Aging 2012;33:2506–2520.
19. Premi E, Cauda F, Gasparotti R, et al. Multimodal fMRI resting-state functional connectivity in Granulin mutations: the case of Fronto-parietal dementia. PloS One 2014;9:e106500.
20. Lee SE, Khazenzon AM, Trujillo AJ, et al. Altered network connectivity in frontotemporal dementia with C9orf72 hexanucleotide repeat expansion. Brain 2014;137:3047–3060.
21. Toller G, Brown J, Sollberger M, et al. Individual differences in socio-emotional sensitivity are an index of salience network function. Cortex 2018;103:211–223.
22. Bacioglu M, Maia LF, Preische O, et al. Neurofilament light chain in blood and CSF as marker of disease progression in mouse models and in neurodegenerative diseases. Neuron 2016;91:56–66.
23. Boeve B, Bove J, Brannelly P, et al. The longitudinal evaluation of familial frontotemporal dementia subjects protocol: framework and methodology. Alzheimers Dement 2019;16:1–15.
24. Ramos EM, Dokuru DR, Van Berlo V, et al. Genetic screening of a large series of north American sporadic and familial frontotemporal dementia cases. Alzheimers Dement 2020;16:118–130.
25. Miyagawa T, Brushaber D, Syrjanen J, et al. Use of the CDR® plus NACC FTLD in mild FTLD: data from the ARTFL/LEFFTDS consortium. Alzheimers Dement 2020;16:79–90.
26. Trzepacz PT, Hochstetler H, Wang S, et al. Relationship between the Montreal cognitive assessment and mini-mental state examination for assessment of mild cognitive impairment in older adults. BMC Geriatr 2015;15:107.
27. Kaufer DI, Cummings JL, Ketchel P, et al. Validation of the NPI-Q, a brief clinical form of the neuropsychiatric inventory. J Neuropsychiatry Clin Neurosci 2000;12:233–239.
28. Sheikh JI, Yesavage JA. Geriatric depression scale (GDS): recent evidence and development of a shorter version. Clinical gerontologist: the journal of. Aging Ment Health 1986;5:165–173.
29. Rojas JC, Wang P, Staffaroni AM, et al. Plasma Neurofilament light for prediction of disease progression in familial frontotemporal lobar degeneration. Neurology 2021;96:e2296–e2312.
30. Esteban O, Markiewicz CJ, Blair RW, et al. fMRIPrep: a robust preprocessing pipeline for functional MRI. Nat Methods 2019;16:111–116.
31. Pruim RHR, Mennes M, van Rooij D, et al. ICA-AROMA: a robust ICA-based strategy for removing motion artifacts from fMRI data. Neuroimage 2015;112:267–277.
32. Parkes L, Fulcher B, Yücel M, Fornito A. An evaluation of the efficacy, reliability, and sensitivity of motion correction strategies for resting-state functional MRI. Neuroimage 2018;171:415–436.
33. Brown JA, Hua AY, Trujillo A, et al. Advancing functional dysconnectivity and atrophy in progressive supranuclear palsy. NeuroImage: Clinical 2017;16:564–574.
34. Fortin J-P, Cullen N, Sheline YI, et al. Harmonization of cortical thickness measurements across scanners and sites. Neuroimage 2018;167:104–120.
35. Yu M, Linn KA, Cook PA, et al. Statistical harmonization corrects site effects in functional connectivity measurements from multi-site fMRI data. Hum Brain Mapp 2018;39:4213–4227.
36. Zhou J, Gennatas ED, Kramer JH, et al. Predicting regional neurodegeneration from the healthy brain functional connectome. Neuron 2012;73:1216–1227.
37. Zhou J, Greicius MD, Gennatas ED, et al. Divergent network connectivity changes in behavioural variant frontotemporal dementia and Alzheimer's disease. Brain 2010;133:1352–1367.
38. Brown JA, Deng J, Neuhaus J, et al. Patient-tailored, connectivity-based forecasts of spreading brain atrophy. Neuron 2019;104:856–868.
39. Trojsi F, Esposito F, de Stefano M, et al. Functional overlap and divergence between ALS and bvFTD. Neurobiol Aging 2015;36:413–423.
40. Farb NAS, Grady CL, Strother S, et al. Abnormal network connectivity in frontotemporal dementia: evidence for prefrontal isolation. Cortex 2013;49:1856–1873.
41. Rytty R, Nikkinen J, Paavola L, et al. GroupICA dual regression analysis of resting state networks in a behavioral variant of frontotemporal dementia. Front Hum Neurosci 2013;7:461.
42. Filippi M, Agosta F, Scola E, et al. Functional network connectivity in the behavioral variant of frontotemporal dementia. Cortex 2013;49:2389–2401.
43. Buckner RL, Andrews-Hanna JR, Schacter DL. The brain's default network: anatomy, function, and relevance to disease. Ann N Y Acad Sci 2008;1124:1–38.
44. Andrews-Hanna JR, Reidler JS, Sepulcre J, et al. Functional-anatomic fractionation of the Brain's default network. Neuron 2010;65:550–562.
45. Hefti MM, Farrell K, Kim S, et al. High-resolution temporal and regional mapping of MAPT expression and splicing in human brain development. PloS One 2018;13:e0195771.
46. Brion J-P, Smith C, Couck A-M, et al. Developmental changes in τ phosphorylation: fetal τ is transiently phosphorylated in a manner similar to paired helical filament-τ characteristic of Alzheimer's disease. J Neurochem 1993;61:2071–2080.
47. Rohrer JD, Ridgway GR, Modat M, et al. Distinct profiles of brain atrophy in frontotemporal lobar degeneration caused by progranulin and tau mutations. Neuroimage 2010;53:1070–1076.
48. Whitwell JL, Weigand SD, Boeve BF, et al. Neuroimaging signatures of frontotemporal dementia genetics: C9ORF72, tau, progranulin and sporadics. Brain 2012;135:794–806.
49. Chen Q, Boeve BF, Senjem M, et al. Rates of lobar atrophy in asymptomatic *MAPT* mutation carriers. Alzheimer's & Dementia: Translational Research & Clinical Interventions 2019;5:338–346.
50. Staffaroni AM, Goh S-YM, Cobigo Y, et al. Rates of Brain Atrophy Across Disease Stages in Familial Frontotemporal Dementia Associated With *MAPT*, *GRN*, and *C9orf72* Pathogenic Variants. JAMA Netw Open 2020;3:e2022847.